

**EFFECT OF IRON CONTENT ON OLIVINE VISCOSITY AND IMPLICATIONS FOR THE MARTIAN MANTLE.** P. Raterron<sup>1,2,3</sup>, C. Holyoke<sup>4</sup>, L. Tökle<sup>2</sup>, N. Hilairt<sup>1</sup>, S. Merkel<sup>1</sup>, G. Hirth<sup>2</sup> and D. Weidner<sup>3</sup>, <sup>1</sup>Unité Matériaux Et Transformations, CNRS, Université de Lille, France (Paul.Raterron@univ-lille1.fr), <sup>2</sup>Dept. of Earth, Environ. & Planet. Sciences, Brown University, RI, <sup>3</sup>Dept. of Geosciences, Stony Brook University, NY, <sup>4</sup>Dept. of Geosciences, University of Akron, OH.

**Introduction:** The upper parts of the mantle of terrestrial planets are olivine-rich, with Fe/(Mg+Fe) ratios (Fe#) lower than ~2% for Mercury, up to 25-30% for Mars, and intermediate compositions for the Earth, the Moon and Venus. Olivine represents more than 60 wt.% of the Martian upper mantle [1], where pressure ( $P$ ) and temperature ( $T$ ) reach 13.5 GPa and 1700 K at 1100-km depth. Results from experiments carried out at low pressure (~0.3 GPa) indicate that increasing Fe content dramatically decreases olivine viscosity [2]. These data suggest that the Martian upper mantle may be ~10 times less viscous than the Earth's at the same conditions. Whether such a weakening occurs at the high pressures relevant to Mars interior is unknown.

Beside weakening olivine, increasing Fe content increases the sensitivity to stress of olivine plastic response [3], which translates into higher stress exponents in classical power laws such as:

$$\dot{\epsilon} = A\sigma^n fO_2^m \exp\left(-\frac{E^* + PV^*}{RT}\right) \quad (1),$$

where  $\dot{\epsilon}$  is the strain rate,  $A$  is a pre-exponential factor,  $\sigma$  the differential stress,  $fO_2$  the oxygen fugacity,  $m$  is a constant,  $E^*$  the activation energy,  $V^*$  the activation volume which quantifies the effect of pressure on viscosity ( $V^* > 0$  implies an increasing viscosity with  $P$ ), and  $R$  the gas constant. High stress exponents promote high viscosity contrasts between the hot deep upper mantle where small differential stresses are expected (< 1 MPa in the Earth), and the colder shallow mantle where stresses are much higher (~50 MPa at 1 GPa and 1100 K in the Earth). Large  $V^*$  increase further the viscosity contrast, since they promote a dramatic decrease in creep rates with increasing pressure.

Moderate viscosity variations, i.e. typically within 1.5 order of magnitude throughout the Martian mantle, dramatically affect the planet thermal history and surface structures [4], and can even promote a Degree-1 convection - which could explain Mars' hemispheric dichotomy. It is, thus, critical to investigate the effect of Fe on olivine viscosity and stress sensitivity at the  $P$ - $T$  conditions relevant to the Martian mantle. Here we show results from deformation experiments performed at high  $P$  on olivine polycrystals with different iron contents, leading to new estimates of the viscosity contrasts expected in the Martian upper mantle.

**Experiments:** deformation experiments were carried out in axisymmetric compression in the Defor-

mation-DIA apparatus (D-DIA) coupled with synchrotron radiation [5], on olivine specimens ~1 mm in length with Fe# ranging from 0 (pure forsterite, Fo100) to 100% (pure fayalite, Fa100). The explored  $P$  and  $T$  ranges were 2.5 – 8.0 GPa and 1073 – 1573 K, and strain rate was in the range  $0.2 - 14 \times 10^{-5} \text{ s}^{-1}$ .

**Starting materials and cell assembly.** Specimens were prepared either by grinding synthetic single crystals of pure forsterite (Fo100) or natural gem-quality single crystals of San Carlos (SC) olivine (Fa10), or synthesized in controlled atmosphere furnaces at Stony Brook University and Brown University as powders of Fa30, Fa50, Fa70 and Fa100 with respective Fe# of 30%, 50%, 70% and 100%. The powders were dry and kept in an oven at 120°C before loading into the high-pressure device. Powders with different iron contents were stacked in two layers into the deformation-cell compression column, and chemically separated from each other by a Ni disk. In some experiments, they were placed inside a Ni Jacket to control  $fO_2$  during deformation. We used the D-DIA dry hybrid cell (Fig. 1), which has been described in details elsewhere [6].

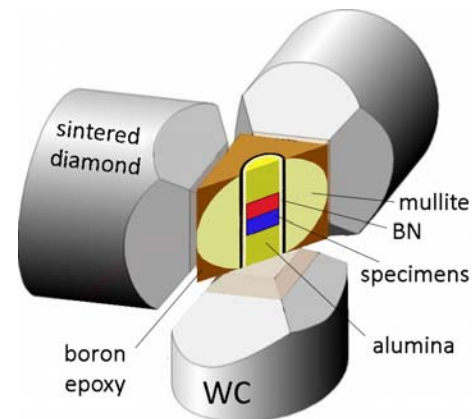


**Figure 1.** Schematic cross section of the D-DIA cubic cell (6-mm in edge). Three of the 6 D-DIA anvils, made of WC or sintered diamond, are represented. Specimens and Ni capsule are placed in-between two alumina pistons inside a BN sleeve, itself placed into a graphite sleeve (the heater, black).

**High-pressure deformation experiments.** Experiments were carried out at the NSLS X17B2 beamline (BNL, Upton, NY), the ESRF ID06 beamline (Grenoble, France) and the APS 6BM-B beamline (ANL, Argonne, IL). Cell assemblies were loaded into the D-DIA and compressed to the desired pressure, then an-

nealed at 1100° or 1200°C for ~1 hour in order to relax the internal stress resulting from cold compression, and sintered the specimens into well-equilibrated polycrystals. Specimens were then deformed at constant strain rate by advancing both D-DIA vertical anvils. Strain rates and applied stresses were measured in situ by X-ray synchrotron imaging and diffraction, i.e., respectively by time-resolved radiography and by comparing  $d$ -spacing of crystallographic planes in different orientations with respect to the principal stress direction. These techniques, coupling high- $P$  deformation devices with X-ray synchrotron radiation, have been described in details elsewhere [7]. Several steady-state deformation conditions (i.e. constant strain rate and stress) were achieved in each experiments, in order to constrain olivine stress exponent  $n$  (stress-step experiment) and/or activation volume  $V^*$  (pressure-step experiment) as a function of iron content.

**Results:** Figure 2 shows a typical strain versus time curve obtained during deformation of a SC olivine specimen together with a Fa50 specimen. Both specimens (stacked such that the sample axes are parallel to the shortening direction) experienced the same  $P$ ,  $T$  and differential stress conditions during the run.

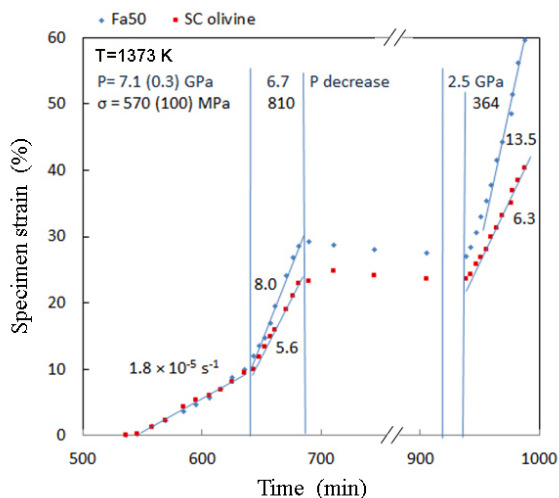


**Figure 2.** Strain versus time curve during run RWD\_41 at the indicated  $P$ ,  $T$  and stress conditions. Specimen strain rates (slopes) are indicated in  $10^{-5} \text{ s}^{-1}$ . SC olivine and Fa50 viscosity contrast is lower than a factor 2.1 at run conditions. Yet, Fa50 strain rate is more sensitive to stress and  $P$  variations than SC olivine strain rate.

Hence, comparing their strain rates (slopes on Fig. 2) allows direct comparison of their effective viscosity. SC olivine and Fa50 exhibit a much smaller viscosity contrast at high pressure (less than a factor of 2.1 in Fig. 2) than the factor of 75 reported at low  $P$  [2]. Furthermore, the strain rate for Fa50 is more sensitive to stress and pressure variations than that for SC oli-

vine. Assuming  $n = 3.5$  and  $V^* = 13 \text{ cm}^3/\text{mol}$  [8] for SC olivine, we obtain  $n \sim 4.6$  and  $V^* \sim 19 \text{ cm}^3/\text{mol}$  for Fa50. The  $n$  values extracted from our high- $P$  experiments are plotted in Figure 3 as a function of Fe content in olivine. These values are consistent with those previously reported for olivine single- and polycrystals, and show an increase of  $n$  (Eq. 1) with increasing Fe#, from  $n \sim 2.7$  for Fe-free olivine to  $\sim 4.5$  for Fa50, with a plateau at  $n \sim 4.5$  for higher Fe#.

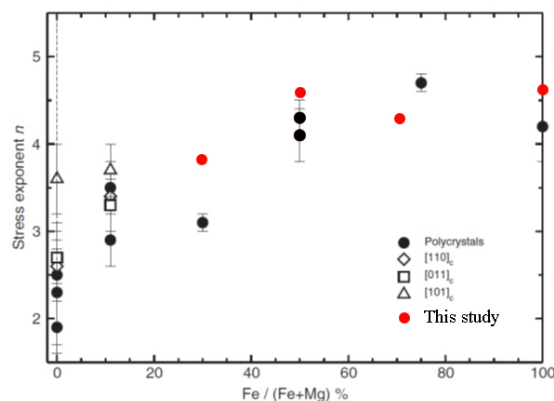


**Figure 3.** Stress exponent  $n$  (Eq. 1) versus Fe# for olivine polycrystals, and single crystals deformed in the indicated orientations [3]. Superimposed are estimates extracted from some of our bi-specimen high- $P$  experiments (red circle).

We conclude that  $n \sim 3.8$  is a reasonable estimate for Fa30, which is a good representative of Fe-rich Martian olivines. Similar considerations lead to the activation volume  $V^* \sim 16 \text{ cm}^3/\text{mol}$  for Fa30. Using  $E^* = 530 \text{ kJ/mol}$  for Fa30, as reported for creep in dry SC olivine [9], and assuming reasonable  $P$ ,  $T$  and stress conditions (c.f., Introduction) and a constant  $fO_2$  in Mars interior, we obtain a viscosity contrast of about  $\times 2740$  throughout the Martian upper mantle, with an increasing viscosity with depth. For comparison, the same calculation for SC olivine leads to a viscosity contrast of only  $\times 67$ , while both Earth's and Mars' shallow mantles have comparable viscosity (within a factor of  $\sim 2$ ). Such a difference between Earth and Mars upper-mantle viscosity variation with depth may promote different convection modes.

**References:** [1] Khan A. and Connolly J. A. D. (2008) *JGR*, 113, E07003. [2] Zhao Y.-H. et al. (2009) *EPSL*, 287, 229-240. [3] Bollinger C. et al. (2015) *PEPI*, 240, 95-104. [4] Roberts J. H. and Zhong S. (2006) *JGR*, 111, E06013. [5] Wang Y. et al. (2003) *Rev. Sci. Instrum.*, 74(6), 3002-3011. [6] Durham W. B. et al. (2009) *PEPI*, 172, 67-73. [7] Raterron P. and Merkel S. (2009) *J. Synchrotron Rad.*, 16, 748-756. [8] Bollinger C. et al. (2014) *PEPI*, 228, 211-219. [9] Hirth G. and Kohlstedt D. (2003) *Geophys. Monograph* 138, 83-105.